Dokuz Eylül Üniversitesi Mühendislik Fakültesi Fen ve Mühendislik Dergisi
Dokuz Eylul University Faculty of Engineering Journal of Science and Engineering

Basılı/Printed ISSN: 1302-9304. Elektronik/Online ISSN: 2547-958X

Aerodynamic Analyses of an Integrated Low-Pressure Compression System for Adaptive-Cycle Micro Turbofan Type Jet Engine

Değişken Çevrimli Mikro Turbofan Jet Motoru için Bütünleşik Düşük Basınç Kompresor Sisteminin Aerodinamik Analizleri

M. Tayyip Gürbüz [1*], Sercan Acarer [2]

[1] İzmir Ekonomi Üniversitesi, Mühendislik Fakültesi, Havacılık ve Uzay Mühendisliği Bölümü, İzmir, TÜRKİYE
[2] İzmir Katip Çelebi Üniversitesi, Mühendislik ve Mimarlık Fakültesi, Makine Mühendisliği Bölümü, İzmir, TÜRKİYE
*Sorumlu Yazar / Corresponding Author **: mtayyipgurbuz@gmail.com

Geliş Tarihi / Received: 13.01.2022 *Araştırma Makalesi/Research Article*
Kabul Tarihi / Accepted: 10.06.2022 *DOI:10.21205/deufmd.2022247222*
Atıf şekli/ How to cite: GÜRBÜZ, M.T., ACARER, S.(2022). Aerodynamic Analyses of an Integrated Low-Pressure Compression System for Adaptive-Cycle Micro Turbofan Type Jet Engine. DEÜ FMD 24(72), 939-951.

Abstract

Unmanned Aerial Vehicles (UAVs) are commonly propeller-driven and low-speed. The concept of cost-efficient, much higher speed and longer range applications of micro jet engines was previously addressed such that an existing basic turbojet engine was converted into a single spool turbofan without using additional components of booster and low pressure turbine. Normally, this situation emerges matching problems since two spools are required to adjust the fan speed independently. A simple solution was to use a Continuously Variable Transmission (CVT) gearbox to adjust optimal speed for the fan. As a result, missing of the positive functionality of the booster would lump into the fan root to form a unified low pressure compression system (unified-LPC). Such a unified-LPC demands unique characteristics of having an extreme twist, very high pressure ratio and mass flux at the root section than at the tip section, despite the exact opposite is being enforced due to the wheel speed rise with radius. In light of these challenges, this work aims to investigate detailed aerodynamics of an existing design previously made and reported by the authors. It is shown that, despite the aerodynamic loading contrast throughout the span, the unified-LPC can still have a wide operating range and acceptable off-design aerodynamics. Complementing the previous design-oriented work, this paper aims to provide guidelines for such unified compression systems.

***Keywords:**, Fan, turbomachinery, variable-cycle, turbofan, CFD, UAV*

Öz

İnsansız Hava Araçları (İHA'lar) genellikle pervaneli ve düşük hızlıdır. Mikro jet motorlarının düşük maliyetli, çok daha yüksek hızlı ve daha uzun menzilli bir konsepti, daha önceki çalışmalarda, mevcut bir temel turbojet motorunun, ek güçlendirici kompresör ("booster") ve düşük basınçlı türbin kullanılmadan tek milli bir turbofana dönüştürüleceği şekilde ele alınmıştı. Normalde bu durum, fan hızını bağımsız olarak ayarlamak için iki mil gerektirdiğinden eşleşme sorunları ortaya çıkarır. Bir

çözüm, fan için optimum hızı ayarlamak üzere Sürekli Değişken Şanzıman (CVT) dişli kutusu kullanmaktır. Sonuç olarak, güçlendirici kompresörün olumlu işlevselliğinin eksikligi, tek fan kademesi içerisinde fiili bir birleşik bir düşük basınçlı sıkıştırma sistemi (birleşik DBK) oluşturmak için fan köküne eklenecektir ve bu da fana ek yük bindirecektir. Böyle bir birleşik DBK, yarıçapla birlikte çark hız artışı nedeniyle tam tersinin fiziksel olarak dikte edilmesine rağmen, kökte uca kıyasla çok yüksek basınç oranı ve kütle akışına sahip olma ve aşırı bir bükülme gibi benzersiz özellikler gerektirir. Bu zorlukların ışığında, bu çalışma, yazarlar tarafından daha önce yapılmış ve rapor edilmiş mevcut bir tasarımın ayrıntılı aerodinamiğini araştırmayı amaçlamaktadır. Kanat uzunluğu boyunca aerodinamik yükleme kontrastına rağmen, birleşik DBK'nın hala geniş bir çalışma aralığına ve kabul edilebilir tasarım dışı aerodinamiğe sahip olabileceğini gösterilmiştir. Önceki tasarım odaklı çalışmayı tamamlayan bu makale, bu tür birleşik sıkıştırma sistemleri için tasarımcılara kılavuz sağlamayı amaçlamaktadır.

Anahtar Kelimeler: *Fan, turbomakinalar, değişken çevrim, turbofan, HAD, İHA*

1. Introduction

Unmanned Aerial Vehicles (UAV) are commonly known and used in recent years. The research studies about them are progressively being increased due to their several advantages such as remote control by human or autonomous control by onboard computers and sustained level flights. Their propulsion technology is generally utilized from reciprocating engine which drives a propeller. This engine is the key elements of recent UAV propulsion technology in order to develop efficient aerial vehicles. There are many research studies considering reciprocating internal combustion engines for UAV propulsion [1,2,3]. The studies carried out and demonstrated innovative concepts with hybrid alternative power sources. Many improvements have been achieved in respect to weight, SFC (Specific Fuel Consumption), heat and noise signature levels. Although these studies have been made a great progress in UAV propulsion, the technology still demands further development in the field that the majority are low speed applications within a limited efficiency levels. Besides, reciprocating engines are not suitable for high-speed flights that severe vibrations happen in engine components with high level of noise and excessive heat release. Therefore, future UAV applications require more advanced propulsion technology which provides high-speed flights, long-range capability and low-cost applications for combat, rescue and surveillance in risky and hazardous environments. To achieve long range flight and high speeds over UAVs, micro-scale turbojet engine design and its integration was investigated by some researches [4,5]. However, the main challenge for turbojets from small-scales to larger platforms is its inefficient off-design performance and poor fuel consumption rates.

As an alternative, larger platforms with improved performance characteristics also corresponding to efficient fuel burn, turbofans which are derived from the turbojets are highly demanded. There are many research fields focusing on turbofans to obtain more efficient and optimized designs with numerous research efforts for decades. One of the main obstacles for such a complex structure is its aerodynamical and thermomechanical conformity and matching for each component. Especially, undesired tip leakage phenomenon has a great impact on overall performance, specifically in SFC of the engine. In this direction, a global optimization study coupling with 3D transient numerical solutions of a turbofan structure [6] focused on minimizing tip leakage flow effect of high pressure compressor. The multidisciplinary optimization of whole-engine achieved 3.44% improvement on SFC of the test engine.

Bypass nozzle area control option on turbofans has also significant effect for overall engine performance. Efficient fuel burn corresponding to reduced SFC could be achieved by applying variable bypass nozzle on a turbofan arhitecture. A study [7] showed that using such a nozzle configuration reduced fuel consumption by 10% at take-off and 2% during cruise condition. This concept also improved aeroacoustic performance as reducing the level of noise about 1 to 2 dB for different operating conditions.

There are further efforts to develop eco-friendly core engine concepts for the future emission goals within NEWAC Framework (New Aero-

engine core concepts) [8,9]. One of the main focus of these efforts is on Intercooled Recuperative Core concepts. Xu et al. [10] examined the effect of recuperator and intercooling combination in a turbofan engine by an extensive optimizer considering performance maps, recuperator and intercooling losses, take-off, cruise conditions and more of them. The resulted SFC improvement was 5.56% for this engine consept comparing to conventional design. It was achieved by modifying fan, compressor and LPT (low pressure turbine) design.

For future emissions goals, another focus of these efforts is on active core structures applicable with geared turbofan engines (GTF) for long range applications. Kyprianidis et al. [11,12] proposed intercooled core engine cycle combined with geared fan and increased Overall Pressure Ratio (OPR) in order to provide 2020 service entry requirements for eco-friendly engines. Focusing on SFC improvement by emissions reduction and engine structure weight and drag issue, intercooled core with GTF engine showed a potential to reach the future goals.

Ultra-high-bypass ratio or open rotor aero engine also known as contra-rotating engine concept was the other concept for NEWAC framework. This concept was detailly investigated by the NASA research team with respect to its off-design performance and engine weight. Then, the results were compared to GTF and direct-drive Turbofan concepts [13]. Although, open rotor engine was much heavier (because of the open rotor's weight and size) comparing to GTF and direct-drive turbofan, the SFC reduction was around 13% at the highest altitude (10000 m) and around 42% at sea level.

Most of the gas turbine engine types have been shown significant imrovements with respect to off-design performance and overall efficiency especially in the recent years, yet micro-scaled gas turbine (under 2 kN of thrust) is the only one have been left to be investigated. In the market search, application of gas turbines for UAV propulsion technology is generally restricted by reciprocating and turbojet engines without advanced micro-scaled turbofans [14].

Considering these challenges and the gap on the field, an existing micro-turbojet was converted into a single spool turbofan without using additional booster and low-pressure turbine (LPT). To adjust the fan speed independently, a CVT gearbox was used. As a result, missing of the positive functionality of the booster was integrated into the fan root to form a unified fan and booster, in other words unified low pressure compression system (unified-LPC). The proposed model is a single stage axial compressor. Previous studies investigated this proposed concept from thermodynamic [14] and three-dimensional on-design perspective [15].

1.1. Motivation

In this study, this unique unified-LPC system is detailly investigated from aerodynamical aspect. The former studies by the authors or their collaborators [14, 15] focus on the thermodynamic performance, feasibility (the former) and detailed design of such a unified-LPC (the latter) by an in-house axisymmetric through-flow design tool [16] and CFD simulations towards 3D design of the fan. As a complementary effort, this study examines its distinctive aerodynamic characteristics much more in detail, especially in off-design conditions, computational fluid dynamics (CFD) simulations, therefore aiming to provide guidelines for future designers.

2. Experimental Validation of the Utilized Solver

The simulations are carried out by ANSYS CFX 18.2 solver and the meshing is performed by ANSYS Turbogrid, which is a structured meshing tool for turbomachinery [15]. Shear Stress Transport (SST) turbulence model with transition modeling is used. Second order accuracy is empoyed for the discretization of all variables. Steady-state approach with mixing plane is applied for temporal modeling. The validation of the solver was performed extensively in the previous study and readers are referred to reference [15] for further details.

3. Aerodynamics and Off-design Performance Investigation

In this section detailed aerodynamics and off-design performance of the novel unified-LPC system was presented. The design point was determined as near choke condition so as to create a better stall margin [15]. The performance maps of core and bypass streams obtained by the previous study [15] are represented in Figure 1.

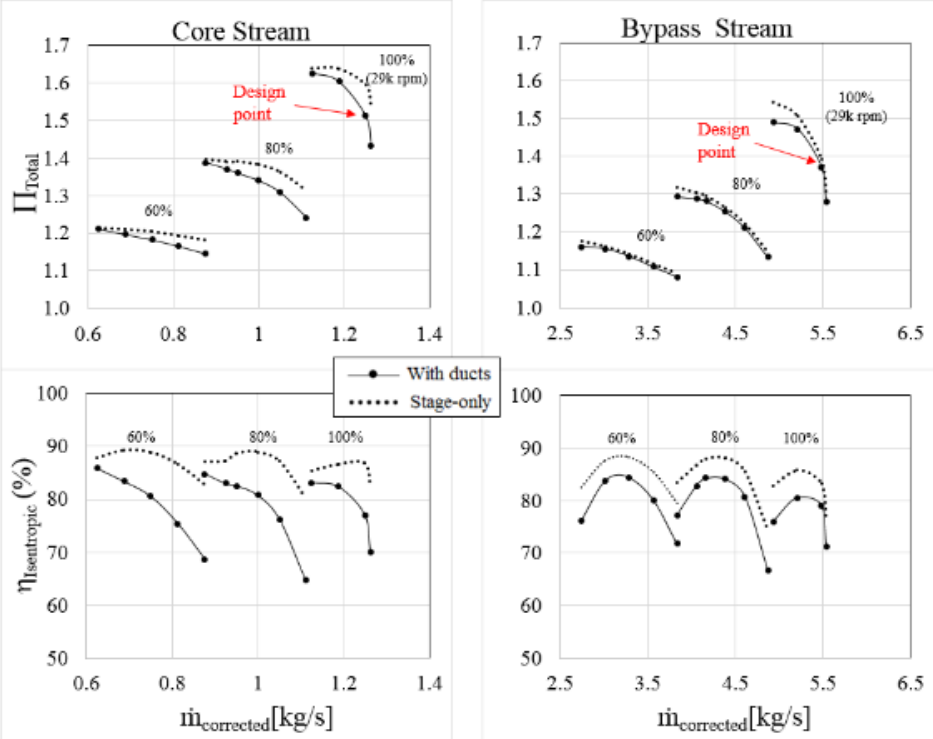

Figure 1. LPC system off-design performance maps[15]

In Figure 1, including nominal (take-off) speed (29000 rpm), low speed performance maps (60% and 80% of the nominal speed) were also presented. The calculated results were obtained for a constant bypass ratio of 4.38 that was determined in the previous work [15]. The maps were presented for both stage-only section considering downstream near stator TE, and stage+ducts considering mixing loss, core and bypass duct losses. Including non-optimized duct shapes, the performance results might not be properly evaluated at off-design condition. Optimized duct shapes (primarily core duct) could reduce the duct losses. In Figure 1, the design point is near choke condition as it was intended in the preliminary design step. This design point (at take-off) corresponds approximately 20% stall margin defined by GE (General Electric) [17] and acceptable 15% stall margin defined by N.A. Cumpsty [18]. These definitions for stall-margin also include the downstream duct losses. Stall margin values indicate that the operating range was improved in return for slight efficiency reduction.

LPC system velocity streamlines can be seen in Figure 2. The streamlines demonstrate a typical turbomachinery stage flow behaviour through the rotor and the stator blades. The flow stream is smoothly seperated to each duct due to the diffuser structure.

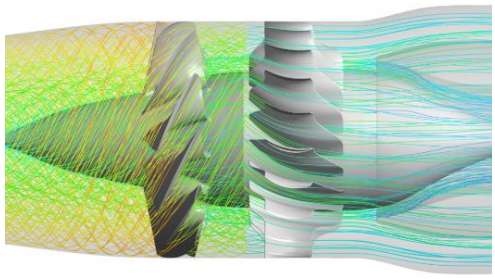

Figure 2. LPC system velocity streamlines

Detailed aerodynamics off-design investigation of the LPC was demonstrated with respect to rotor and stator blades. In Figure 3, blade-to-blade relative Mach distribution for three operating conditions. These conditions are near-stall, design point, near-choke at nominal speed

(29000 rpm) that is shown from near-hub to near-tip.

The shock formations for all three operating conditions at 0.9 span confirm the demonstration of Biollo's [19] shock structure formations. The shock is formed upstream of the blade and it is less inclined to incoming flow at the stall condition. Because lower mass flow rates and higher incidence make the shock less inclined. The shock structure at the choke condition develops furher shock downstream of the main shock and it is more inclined to the incoming flow. However, the design condition shock formation should normally create one main shock which should bifurcate to incoming flow at the leading edge. Instead, the main shock creates another further but weaker secondary shock near the trailing edge suction side as it only happens in choke operation. The reason is that the selected design point of the LPC (see Figure 1) is close to the choke point.

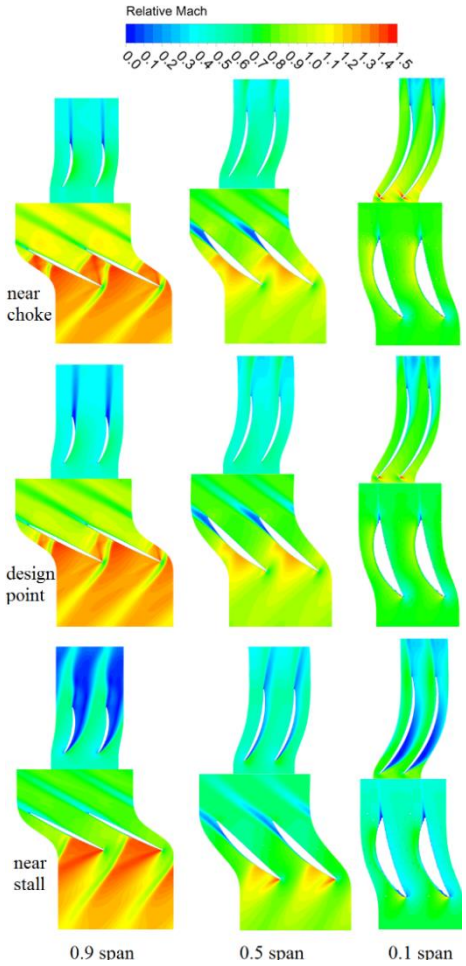

Figure 3. Relative Mach distribution for three operating conditions; near-choke (top), design point (mid), near-stall (bottom)

At design point, near hub (0.1 span) there is a spike (local acceleration) both for rotor and stator leading edges. The spike is stronger at the stator leading edge for near-choke and creates a passage shock there. This situation is normal and it is not possible to avoid due to the circular leading edge shape. The sudden acceleration is the result of a dramatic increase of the local static pressure just after the leading edge of the rotor and the stator (see Figure 4). There is also a low-momentum region through the trailing edge which induces downstream mixing losses. Near hub, this low-momentum region is much bigger for near-stall operation and smaller for near-choke operation. The flow seperates from the leading edge of the stator and creates a very

large seperation bubble for near-stall condition near hub. Meanline blade-to-blade view shows two acceleration zone at the rotor suction side for design point. It does not have a major effect on the performance and could be avoided with a further design optimization. However, this situation creates a shock formation at the leading edge for near-stall condition and for near-choke, the second acceleration zone creates a passage shock formation. There is a flow seperation at the trailing edge of the stator due to the tip leakage flow influence for both design and near-choke condition. At the design step, relaxed tip design with a reduced inlet Mach (~0.5) makes this situation unavoidable. Furthermore, near-stall operation, the suprising thing about the stator tip is that there is a complete stall, yet it takes the least attention at the design step. Increasing the solidity or lower incidence angle would be a solution to avoid this issue. However, these solutions could reduce the design point efficiency.

In Figure 4, chordwise static pressure distribution for three operating conditions are shown for the nominal speed of 29000 rpm. The first noticeable thing in the figure is that the static pressure trend of design point and near choke condition shows considerable increase between 0.6 and 0.9 streamwise locations. It is the reason of the double shock structure formation at the near-tip region which can also be seen in Figure 3. The shock structures are clearly visible on blade surface with red dashed-lines in Figure 5. The second shock of the design point is weaker than the near-choke and it reflects its impact with relatively small static pressure rise (see Figure 4). Another important thing, the overall blade loading is getting higher from near-choke to near-stall condition. At near-stall, this trend increases the unsteadiness of fan rotor. However, it is a normal behaviour for such a transonic rotor blade. In Figure 4, at the trailing edge of the rotor and the stator (near 1.0 chordwise position), a flow migration happens from pressure side to suction side which is a common and an unavoidable aerodynamic phenomenon for turbomachinery blades.

Figure 5 demonstrates the distribution of static pressure on the rotor blade surface both for Suction Side (SS) and Pressure Side (PS) at nominal speed. The red-dashed-lines represent the shock formation through different operating conditions. The boundary of the shock is becoming thicker from near-stall to near-choke condition. There is a local static pressure rise near the SS leading edge (mid to tip region) both for near-choke and design point operations. Since, relatively higher angle of attack for the rotor blade tip region makes the flow quasi-stagnated. For the near-stall operating condition the longest radial shock formation is observed. It causes a bigger flow seperation zone (see Figure 6) and rises the static pressure and therefore loading towards the trailing edge (see Figure 5). Besides, the tail of the shock to the blade root contributes further downstream blade loading.

Nominal speed suction side blade surface velocity streamlines are presented in Figure 6 for different perspectives. Strong radial fluid migration schemes are observed as the flow interacts with the shock. The shock structure creation gives rise to low momentum fluid accumulation at the tip region which is known to be detrimental for a stable operation. It also causes thicker boundary layer to induce further blade wake development. Therefore, the seperation lines reaching the tip region are an indication of the shock formation.

The seperation line due to the shock formation is followed by a reattachment line. The reattachment of the flow is relatively delayed for the near-stall operation with reference to design point.

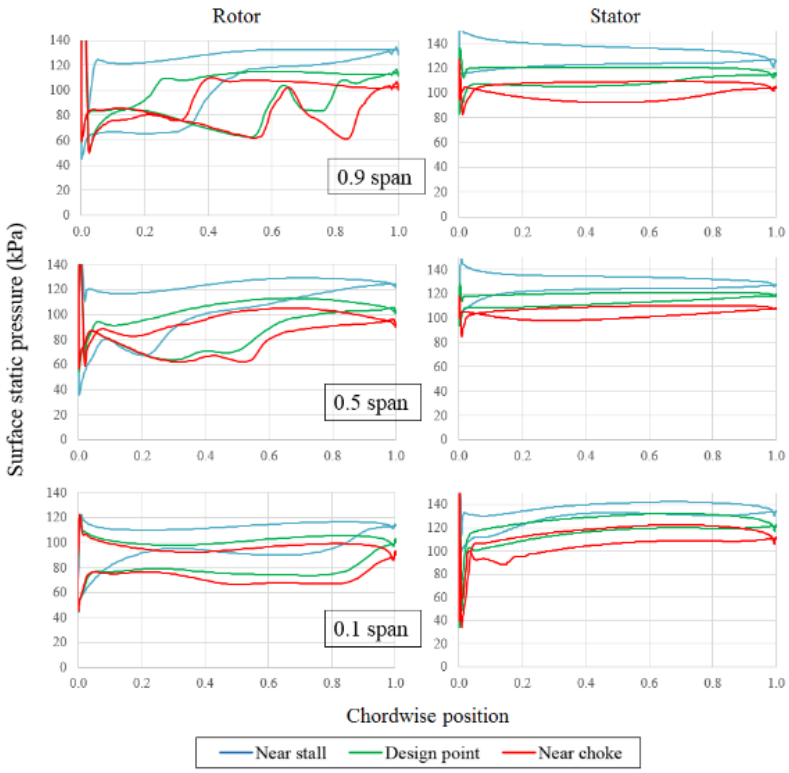

Figure 4. Static Pressure chordwise distribution for 0.9 (top), 0.5 (mid), and 0.1 (bottom) spans

There is a midspan seperation zone for near-choke and design point conditions (see Figure 6). The seperation zone is relatively weak for design operation and the flow reattachment is provided near the seperation. The reason of this phenomenon is the blade over curved geometry to provide highly loaded blade characteristics. Moreover, seperation vortex occurs for both operating conditions. This phenomenon is the result of seperation zone interaction with the corner stall seperation. Near-stall operation, the corner stall seperation is longer reaching the midspan region. The corner stall seperation also induces the reverse flow for the design point and near-choke condition. As it is seen in Figure 6, reverse flow bifurcates and one side interacts with the seperation vortex as mentioned, one side migrates above because of the midspan trailing edge extreme curvature. This migration even reaches near tip region at the near-choke condition.

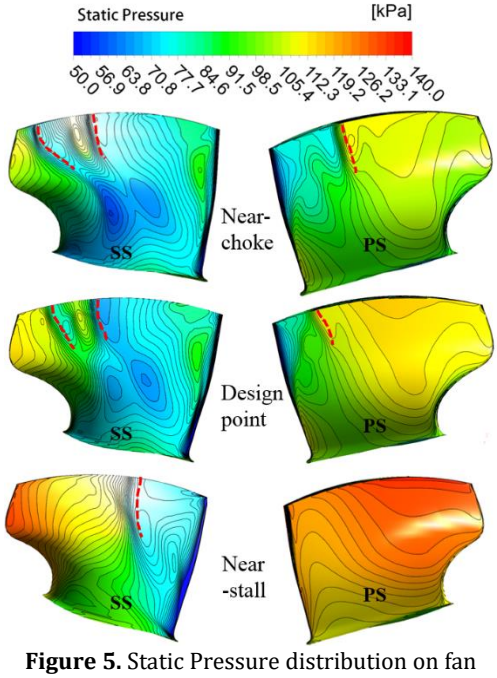

Figure 5. Static Pressure distribution on fan rotor for different operating conditions

In Figure 6, leading edge DCA (double circular arc) shape delays flow reattacment. The DCA is not suitable for subsonic flows and it creates leading edge spike that is a common phenomenon for this profile. As a result, the reattachment zone is obvious until 0.7 span blade profile where it begins to become supersonic. Around tip, blade supersonic profile with sharp edges, there is no delay for the flow attachment.

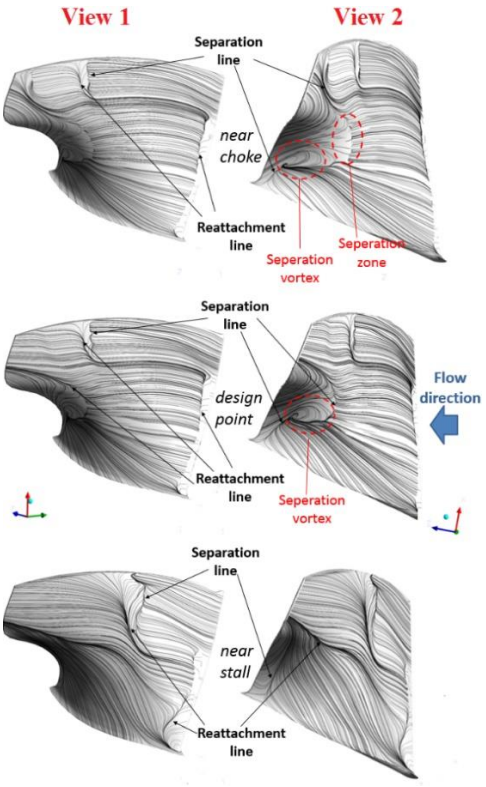

Figure 6. Three operating point streamlines on rotor blade suction side from different perspectives, View 1 (left), View 2 (right).

Figure 7 shows streamwise absolute Mach distribution (in stationary frame) for design point and near-stall operation at nominal speed. In Figure 7, relatively thicker wake appearance is clearly visible at the downstream of the stator tip. It becomes stronger at near-stall operation causing even a complete flow seperation at the outer duct. The difference of the Mach between upstream and downstream of the stator is clearly visible. This indicates a dramatic deceleration of the flow. Leaned rotor wakes are also demonstrated in the figure with black-dashed circle. The corner flow seperation both for suction side of the stator hub and tip section creates low-momentum zone. The corner flow seperation at the hub is weaker and smaller especially due to rotor hub radius increase (partly in stator hub as well) by providing a convergent shape flowpath. As a result, a mostly attached flow enters the core duct. Even strong wake mixing losses occur downstream of the stator, the flow remains attached. Therefore, the design strategy provides its accuracy.

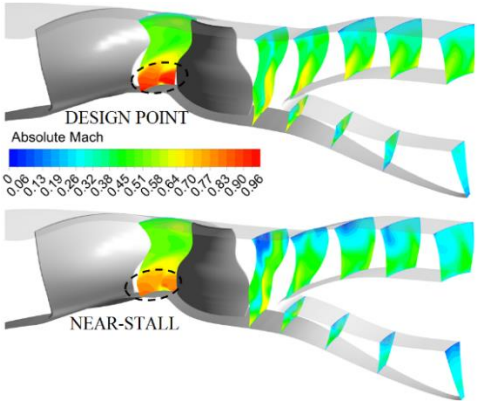

Figure 7. Streamwise absolute Mach distribution at design point (top) and near-stall condition (bottom).

Total pressure distribution through the flowpath is shown in Figure 8. It is interesting that the rotor downstream flow behaviour is formed an S-shaped low pressure zone corresponding to high momentum zone. This form represents the rotor trailing edge leaned S-shape. It is clearly visible in Figure 9 as well. It is the reason of rotor pressure and suction side flow instanteneous encountering and mixing. This phenomenon creates intense flow vortices which is seen in Figure 9 and the flow vorticity charateristics and shear strain rate of the flow show an analogy. In addition, a similar mixing phenomenon also occurs at the stator downstream. Yet, it is weaker and more stable which does not create further intense vorticies and disappears. At the core duct, vorticity characteristics of the flow is very dominant because of the corner stall seperation. However, these vorticies are disappeared near the core duct outlet due to the high diffusivity.

The boundary layer near tip wall is rather thicker because of the tip leakage flow of the rotor. However, it is smootly diffused by bypass duct and became thinner (Figure 7,9).

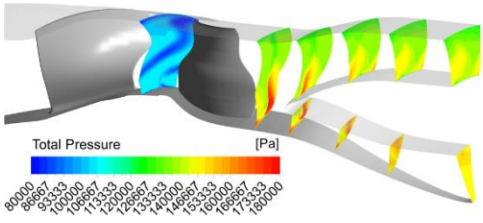

Figure 8. : Streamwise total pressure distribution

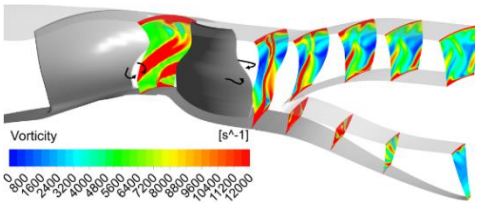

Figure 9. Vorticity of the flow in the streamwise direction (Higher values clipped)

Till now, the off-design results are evaluated by considering nominal shaft speed of 29000 rpm. The lower speed operating conditions of the LPC should also be considered to provide sufficient information about the off-design performance. In Figure 10, blade-to-blade relative Mach distribution is demonstrated for three different shaft speeds (100% nominal speed, 80% speed, 60% speed) which their curves are already presented in Figure 1. It should be mentioned that the figures are taken from the design point for each individual shaft speed. As it is expected, near-tip (0.9 span) shock formation becomes weaker at 80% speed and another acceleration zone (near-sonic) is observed downstream of the shock on the suction side. It can also be observed in Figure 11. The chordwise distribution of the static pressure makes a peak between 0-0.2 chordwise position. This formation becomes weaker at 60% speed near-tip section. There is only a minor acceleration (spike) at the rotor leading edge and no seperation occurs because of the lower mass flow levels. Local acceleration or even a weaker shock formation for lower shaft speeds moves away the design point from choke line. As a result performance curve of lower speeds becomes less inclined to choke line (see Figure 1) and rather widens operating range which is a normal outcome for such a turbomachinery.

In Figure 11, near hub static pressure of the rotor increases between 0.8 and 1.0 chordwise positions for the suction side trends. This situation is the reason of the trailing edge flow seperation which creates a low momentum zone at the rotor suction side. For all three shaft speeds, it is clearly seen at 0.1 span from the Figure 10. This low momentum zone could be eliminated by a relatively moderate convex shape of the suction side or by a wider chord line of the rotor blade. However, these parameters should wisely be considered in the design phase within the whole design perspective.

Another remarkable thing in Figure 10, stator near hub large seperation zone which begins from the leading edge for nominal speed is disappeared at lower shaft speeds. Both for 60% and 80% operating speeds, this low momentum zone migrates downstream of the stator and weakens in point of size and magnitude.

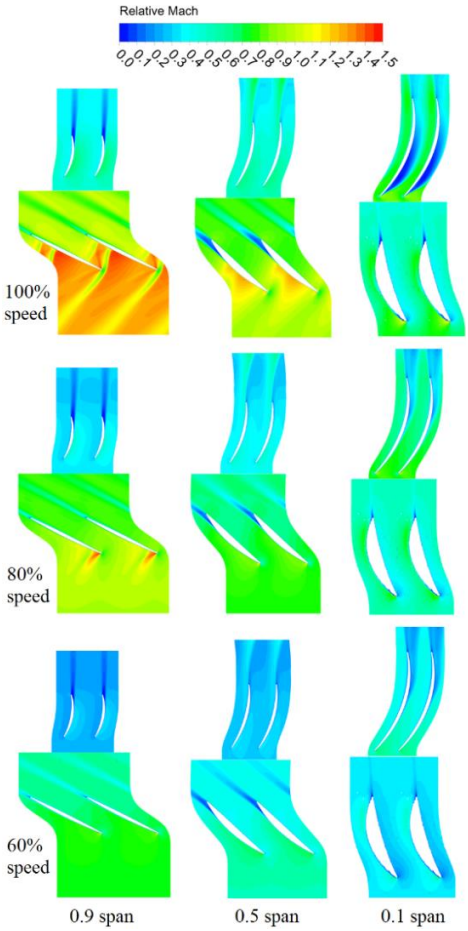

Figure 10. Relative Mach distribution for different shaft speeds; 100% design speed (top), 80% speed (mid), 60% speed (bottom)

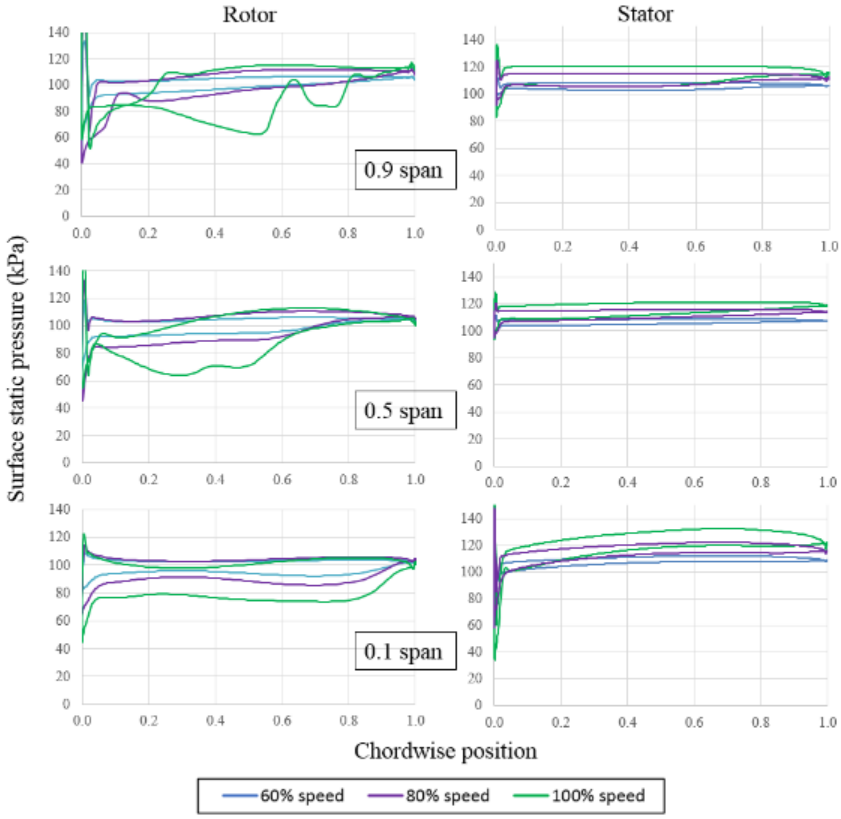

Figure 11. Static Pressure chordwise distribution for 0.9 (top), 0.5 (mid), and 0.1 (bottom) spans

Tip clearance flow behaviour is another crucial factor and should be detailly investigated. Since, pre-design requirements of the LPC were the result of the tip performance deterioration [15]. It is an unavoidable phenomenon for such an unshrouded high speed fan blades and it induces flow instabilities and losses, effecting overall performance negatively. Note that, the rotor tip clearance is 0.25 mm which is approximately 0.5% of the blade span for this fan rotor.

Figure 12 shows near tip (positioned at 98%), relative Mach distribution of the rotor blades. It is seen in the figure that the main shock strongly impacts on the rotor blade suction side at the half downstream region by interacting negatively with the local boundary layer. Then, thickening of the boundary layer happens and a seperation bubble is created because of the adverse pressure gradient scheme across the shock. However, the seperated flow is reattached before trailing edge and avoided further blade wakes. Tip leakage flow also shows itself clearly in the figure. It begins dowstream of the leading edge suction side and creates a tip leakage vortex downstream of the passage flow. Tip leakage vortex firstly encounters with the main shock. It generates low momentum region (by its diffusion inherent characteristics) which is called blockage zone by passing through the adverse pressure gradient due to the main shock [20]. Normally, the blockage zone intends to diffuse further by growing itself. However, it is ceased by the secondary shock-vortex interaction. This time, it becomes stronger downstream due to the secondary shock weaker characteristics. Tip leakage vortex and further weaker downstream tip vortex evaluation from 0.95 span to tip section are presented in Figure 13.

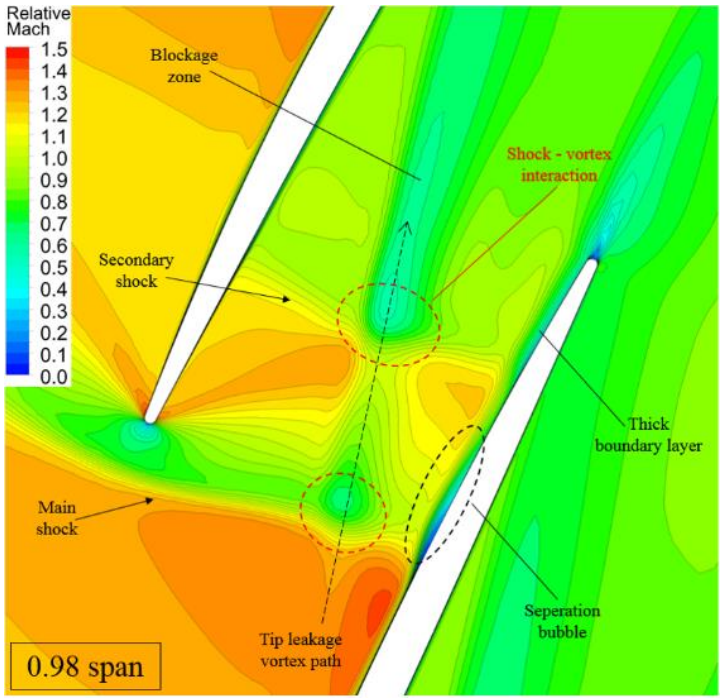

Figure 12. Near tip section (0.98 span) Relative Mach distribution

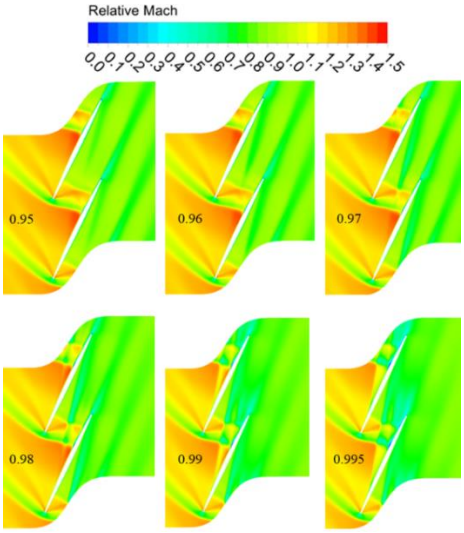

Figure 13. From 0.95 span to 0.995 span tip clearance flow influence

Figure 12 and 13 presented the tip clearance flow phenomenon. Yet, it is a 3D flow behavior and should be properly investigated. Figure 14 demonstrates a typical tip clearance flow occurance and entropy generation at the blade passages.

As it is mentioned in Figure 12, tip leakage vortex generation happens due to the migration of the flow from pressure side to suction side. Suction side regular flow comes across with tip flow migration and as a results this event creates vorticies. These vorticies grown up and become stronger with the interaction of the leakage jet flow through the passage and forms a tip leakage vortex. White dashed arrow line shows the vortex core of the tip leakage vortex. It originates the center of the entropy generation zone. The vortex core diffuses and drives its way slightly to the bottom spans and thickens the boundary layer of the entropy further downstream. However, the diffusion makes the vortex less stronger and reduces the entropy generation (see Figure 14 near trailing edge).

There is also a relatively small entropy generation zone near the suction side blade boundary layer at the tip that is encircled with a white dashed lines. It is possibly occurred due to the scraping vortex formation. Because, the blade rotation is very close to the casing for smaller tip gaps; casing boundary layer is rolled up due to the dominating effect of the blade tip and forms a scraping vortex [21].

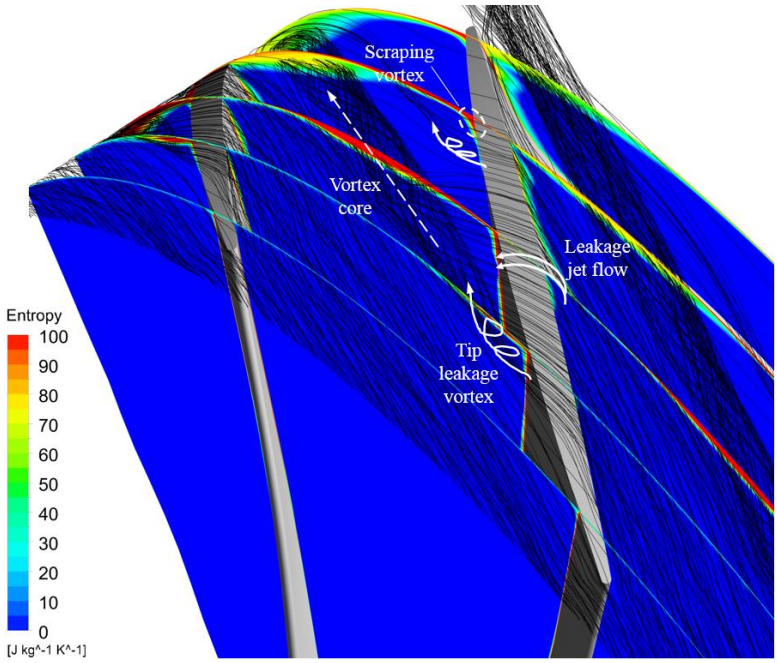

Figure 14. Entropy generation and blade tip flow characteristics (higher values were clipped)

4. Conclusion

A novel unified-LPC system for an adaptive micro-scaled turbofan engine was investigated from aerodynamical perspective. The results show that wider operating range and reasonable off-design performance are preserved, although the design was challenging with a hub-loaded and tip relaxed concept.

As it is expected shock structure on the blade is less inclined at lower mass flows, and as mass flow increases the main shock structure develops further dowstream shock. Flow reattachment is delayed at near-hub region because of the DCA shape. Yet, the seperation vortex becomes thinner with higher loads. On the other hand, the reattachment is provided near sepearation at midspan and tip regions. Furthermore, the shock formation does not penetrate to lower span levels under any operating condition and preserves performance of the LPC.

Another critical issue which is the dramatic change of core duct area is avoided by increasing the the rotor hub diameter. As a result corner flow seperation becomes weaker and prevents larger seperation downstream of the core duct.

As a tip relaxed design, tip leakage vortex occurs downstream of the leading edge and interacts with the shock structure. As a result, it creates a low momentum region. In nature, this region intends to go further downstream. However, as the mass flow increases, the vortex core interacts with a secondary shock. This design strategy weakens the tip leakage vortex formation and prevents further performance deterioration.

In conclusion, aerodynamical investigation of such a LPC design in this study is expected to present a unique and useful guidelines for the future engine applications of UAVs mainly and for the future turbofan engines.

Acknowledgment

This paper was supported by the NATO Science for Peace and Security Programme under grant G5202-Versatile UAV Engine Development and by the U.S. Office of Naval Research Global under award number N62909-17-1-2176.

References

[1] Hooper, P. 2005. Stepped piston engines for multi-fuel UAV application. IMechE Conference on Propulsion Systems for Unmanned Aircraft, 14 April, Bristol, UK.

[2] Lieh, J., Spahr, E., Behbahani, A., & Hoying, J. 2011. Design of hybrid propulsion systems for unmanned aerial vehicles. 47th AIAA/ ASME/ SAE/ ASEE Joint

Propulsion Conference & Exhibit, 31 July - 3 August San Diego, CA, USA.

[3] Cirigliano, D., Frisch, A. M., Liu, F., & Sirignano, W. A. 2017. Diesel, Spark-Ignition, and Turboprop Engines for Long-Duration Unmanned Air Flights. Journal of Propulsion and Power, Vol.34 No.4, pp. 878-892. DOI: 10.2514/1.B36547.

[4] Chiang, H. W. D., Hsu, C. N., Lai, A., & Lin, R. 2002. An investigation of steady and dynamic performance of a small turbojet engine. ASME Turbo Expo 2002: Power for Land, Sea, and Air, 3-6 June, Amsterdam, The Netherlands, 1097-1104.

[5] Collie, W., Burgun, R., Heinzen, S., Hall, C., & Chokani, N. 2003. Advanced propulsion system design and integration for a turbojet powered unmanned aerial vehicle. 41st Aerospace Sciences Meeting and Exhibit 6-9 January. Reno, Nevada, USA.

[6] Toal, D. J., Keane, A. J., Benito, D., Dixon, J. A., Yang, J., ... & Kill, N. 2014. Multifidelity multidisciplinary whole-engine thermomechanical design optimization. Journal of Propulsion and Power, Vol.30 No.6, pp. 1654-1666. DOI: 10.2514/1.B35128.

[7] Michel, U. 2011. The benefits of variable area fan nozzles on turbofan engines. 49th AIAA Aerospace Sciences Meeting including the New Horizons Forum and Aerospace Exposition. 4-7 January 2011, Orlando, Florida, USA. DOI: 10.2514/6.2011-226

[8] Wilfert, G., Sieber, J., Rolt, A., Baker, N., Touyeras, A., & Colantuoni, S. 2007. New environmental friendly aero engine core concepts. XVIII International Symposium of Air Breathing Engines, Sept 2-7, Beijing, China.

[9] Rolt, A. M., & Kyprianidis, K. 2010. Assessment of New Aero Engine Core Concepts and Technologies in the EU Framework 6 NEWAC Programme. ICAS 2010 Congress Proceedings, 19-24 September, Nice, France.

[10] Xu, L., Kyprianidis, K. G., & Grönstedt, T. U. 2013. Optimization study of an intercooled recuperated aero-engine. Journal of Propulsion and Power, Vol. 29, No. 2, pp. 424-432. DOI: 10.2514/1.B34594.

[11] Kyprianidis, K. G., Rolt, A. M., & Grönstedt, T. 2014. Multidisciplinary analysis of a geared fan intercooled core aero-engine. Journal of Engineering for Gas Turbines and Power, Vol. 136, No.1. 011203 (11 pages). DOI: 10.1115/1.4025244.

[12] Kyprianidis, K. G., & Rolt, A. M. 2015. On the optimization of a geared fan intercooled core engine design. Journal of Engineering for Gas Turbines and Power, Vol. 137, No.4, 041201 (10 pages). DOI: 10.1115/1.4028544.

[13] Hendricks, E., & Tong, M. 2012. Performance and weight estimates for an advanced open rotor engine. 48th AIAA/ASME/SAE/ASEE Joint Propulsion Conference & Exhibit, 30 July-1 August 2012, Atlanta, Georgia, USA. DOI: 10.2514/6.2012-3911.

[14] Kadosh, K., & Cukurel, B. 2017. Micro-turbojet to turbofan conversion via continuously variable transmission: thermodynamic performance study. Journal of Engineering for Gas Turbines and Power, Vol. 139, No. 2, 022603 (10 pages). DOI: 10.1115/1.4034262.

[15] İlhan, M., Gürbüz, M. T., & Acarer, S. 2019. Unified low-pressure compressor concept for engines of future high-speed micro-unmanned aerial vehicles. Proceedings of the Institution of Mechanical Engineers, Part G: Journal of Aerospace Engineering, Vol. 233, No.14. DOI: 10.1177%2F0954410019840968.

[16] Acarer, S., & Özkol, Ü. 2019. Off-design analysis of transonic bypass fan systems using streamline curvature through-flow method. International Journal of Turbo & Jet-Engines, Vol. 36, No.2, pp. 137-146. DOI: 10.1515/tjj-2016-0083.

[17] Fowler, T. W. 1989. Jet Engines and Propulsion Systems for Engineers. GE Aircraft Engines, USA.

[18] Cumpsty, N.A. 1989. Compressor aerodynamics. Longman Scientific & Technical.

[19] Biollo, R. (2008). Systematic investigation on swept and leaned transonic compressor rotor blades.

[20] Suder, K. L. 1997. Blockage development in a transonic, axial compressor rotor. ASME 1997 International Gas Turbine and Aeroengine Congress and Exhibition 2-5 June, 1997, Orlando, Florida, USA.

[21] Kumar, A., & Pradeep, A. M. 2018, June. Performance Evaluation of a Tandem Rotor Under Design and Off-Design Operation. In ASME Turbo Expo 2018: Turbomachinery Technical Conference and Exposition, Oslo, Norway 11-15 June.